PCCP

Accepted Manuscript

ROYAL SOCIETY OF CHEMISTRY

www.rsc.org/pccp

Exploring the comparative binding aspects of benzophenanthridine plant alkaloid chelerythrine with RNA triple and double helices: Spectroscopic and calorimetric approach

Lucy Haque, Ankur Bikash Pradhan, Sutanwi Bhuiya and Suman Das*

Department of Chemistry
Jadavpur University
Raja S. C. Mullick Road, Jadavpur
Kolkata 700 032
India

*To whom all correspondence should be addressed.

Tel.: +91 94 3437 3164, +91033 2457 2349

Fax: +91 33 2414 6266

E-mail:

SD: sumandas10@yahoo.com

LH: lucy.haque@gmail.com

ABP: ankurpradhan727@gmail.com

SB: s.bhuiya12@gmail.com

Abstract

A comparative study on the interaction of a benzophenanthridine alkaloid chelerythrine (CHL) with RNA triplex poly(U).poly(A)*poly(U) (here after U.A*U, .(dot) and *(asterisk) represent Watson-Crick and Hoogsteen base pairing respectively) and its parent duplex poly(A).poly(U) (A.U) was carried out by using a combination of various spectroscopic, viscometric and calorimetric techniques. The interaction was characterized by hypochromic and bathochromic effects in the absorption spectrum, increase of thermal melting temperature, enhancement in solution viscosity, perturbation in circular dichroic spectrum. Binding constant calculated by using spectrophotometric data was in the order of 10^5 for both forms of RNA, but it was greater for triplex RNA (30.2×10^5 M^{-1}) than duplex RNA(3.6×10^5 M^{-1}). Isothermal titration calorimetric data are in good agreement with the spectrophotometric data. The data indicated stronger binding of CHL to the triplex structure of RNA compared to the native duplex structure. Thermal melting studies indicated greater stabilization of the Hoogsteen base paired third strand of RNA triplex compared to its Watson-Crick strands. Mode of binding of CHL to both U.A*U and A.U was intercalation as revealed from fluorescence quenching, viscosity measurement and sensitization of fluorescence experiment. Thermodynamic data obtained from isothermal calorimetric measurements revealed that association was favoured by both negative enthalpy change and positive entropy change. Taken together, our results suggest that chelerythrine binds and stabilizes the RNA triplex more strongly than its respective parent duplex. The results presented here may be useful for formulating effective antigene strategies involving benzophenanthridine alkaloids and the RNA triplex.

Keywords: Benzophenanthridine alkaloid, Fluorescence energy transfer, Intercalation, Isothermal titration calorimetry, Triple and double helical RNA.

Introduction

Interaction of small molecules with higher order nucleic acids has been the center of attention since the discovery of triple helical nucleic acid structures.[1] The biological relevance of triple helical nucleic acid structures has been reinforced from the discovery of new triplex-unwinding helicases[2] as well as the increasingly apparent biological roles played by non-coding RNAs.[3] Triple helical forms of DNA and RNA have gained significance over double helical structures for their various potential applications in many cellular processes [4] and in artificial regulation of gene expression by antigene technology, mapping of genomic DNA, and gene-targeted mutagenesis.

Triple helical nucleic acids are produced by sequence-specific binding rules that are different although conceptually similar to the familiar Watson-Crick base-pairing scheme.[5] It is usually formed through the sequence-specific association of a single-stranded homopurine or homopyrimidine triplex-forming oligonucleotide (TFO) with the major groove of a homopyrimidine homopurine stretch in duplex DNA/RNA. In the pyrimidine motif triplex, a homopyrimidine TFO binds parallel to the homopurine strand of the target duplex by Hoogsteen hydrogen bonding to form T.A*T or C.G*C^+ or U.A*U base triplets (the dot represents the Watson-Crick bonding while asterisk has been used for the Hoogsteen ones). On the other hand, in the purine motif triplex, a homopurine TFO binds antiparallel to the homopurine strand of the target duplex by reverse Hoogsteen hydrogen bonding to form A.A*T or G.G*C or A.A*U base triplets.[6] Apart from few cases (Svinarchuk *et al*, 1995),[7] the stability of the triple helices is usually weaker than that of double-helices due to its slow rate of formation (typically three orders of magnitude slower than duplexes) and electrostatic repulsion between three polyanionic strands.[8] The poor stability of the triple helices is a critical limitation in their efficacy and application *in vivo* as probes of structure, inhibitors of protein synthesis as well as therapeutic agents.

Consequently, molecules having the ability to recognize, bind and stabilize specific sequences of triple helices are of particular interest in antigene therapy. Since the discovery of triple helical nucleic acid structures, several studies have been reported on the properties of DNA triple helices[9] and many small molecules that can improve the stability of triplexes have been described.[10-13] Comparatively less studies have been undertaken on the stabilization of RNA triplexes. The complex structure of RNA triplex has been gained considerable attraction over DNA triplex due to its diverse biological functions and its applications in antisense and antigene strategies. A RNA triplex consist of tertiary motif is found in many pseudoknots and other structured RNAs. Basically RNA triplex is formed through the tertiary interaction of RNA duplex and RNA singlet in the major or minor groove of Watson-Crick base paired stem. Naturally occurring triplexes are important for shaping RNAs. Till now biological applications and study of RNA triplex in its early stage. Here we summarize the formation and the experimental methods for characterization of RNA triplex and its interaction with chelerythrine.

Among the nucleic acid binding of small molecules, naturally occurring small molecules have been in the focus of study as therapeutic agents for their high abundance and low toxicity. The alkaloids represent a very extensive group of nitrogen-containing secondary metabolites having wide range of biological activities. A large number of studies on the interaction of different alkaloids with DNA have been reported. Comparatively less attention has been given to alkaloid-duplex RNA interaction and specially alkaloid triplex RNA inteaction. Among the alkaloids, interaction of RNA with β-carboline alkaloids have been reported.[14] In alkaloids, benzophenanthridine group of plant alkaloids have gained the prior attention for their wide range of pharmacological activities.[1516]Among the benzophenanthridine group of alkaloids, sanguinarine is a well studied compound. It shows diverse biological activity as well as strong nucleic acid binding capacity[17]Sanguinarine has

been reported to interact with different polymorphic forms of nucleic acid structures.[18]This compound has been reported to bind strongly with DNA/RNA triple and double helices.[19] Chelerythrine (hereafter CHL, Fig. 1) (1,2-dimethoxy-12methyl[1,3]benzodioxolo[5,6-*c*]phenanthridin-12-ium) is another benzophenanthridine alkaloid, which slightly differs from sanguinarine in the type and position of substituents in the structure. CHL exhibits pronounced cytotoxicity,[16,20,21] anticancer[22,23] and antitumour[23,24] activity. Recent studies have revealed that CHL can exist between iminium form (charged) and alkanolamine form (uncharged) with a pKa of 8.58.[25] There are few studies on the DNA binding of CHL.[26,27] A detail study on the interaction of this compound with DNA has been reported by Basu *et al.*[25] Our laboratory has published the interaction of CHL with single stranded polyriboadenylic acid very recently.[28] However, the studies are so far limited to double helical DNA and single stranded polyriboadenylic acid and no work has been reported so far on the interaction of CHL with double and triple helical forms of RNA. Keeping in view of the diverse biological effects of CHL and importance of structure of RNA triple helices, our aim was to investigate the interaction of CHL with U.A*U RNA triple helix using various spectroscopic and calorimetric techniques. Studies have also been carried out on the interaction of the alkaloid with the parent double helical A.U for a meaningful comparison. Overall, our focus is to elucidate and understand the structural and energetic aspects of CHL binding to the triple and double helical RNA.

Materials and methods

Materials

CHL, A.U and poly (U) were purchased from Sigma Aldrich Corporation (St. Louis, MO, USA). Sodium cacodylate trihydrate was also purchased from Sigma Aldrich Corporation. They were used without further purification. Concentration of CHL was checked spectrophotometrically by using known extinction value of 37060 M^{-1} cm^{-1} at 316 nm.[28] To

avoid light induced photochemical change CHL solutions were kept in dark all time. Molar extinction value of poly(U) and A.U were 9350 and 7140 $M^{-1}cm^{-1}$ at 260 nm respectively.[19] Studies on triple and double helical RNA were carried out in 35 mM cacodylate buffer of pH 6.5 (10 mM cacodylate buffer, 0.1 mM Na_2EDTA, 25 mM NaCl, SCH buffer). Moderate salt concentration was used for the better stabilization of triplex.[29]Millipore filtered water and analytical grade reagents were used for buffer preparation. All the buffer solutions were filtered through Millipore membrane filter of 0.45 μm before use. Under our experimental range CHL was fully in iminium form and no deviation of Beer's law was noted.

Methods

UV-Visible Absorption Experiments

All the UV-VIS absorbance studies were made on a Shimadzu model UV-1800 spectrophotometer (Shimadzu Corporation, Japan) in matched quartz cells of 1 cm path length. A thermo-programmer was attached to it to maintain the temperature of this spectrometer by peltier effect. Spectrophotometric titrations were performed using the methodology described previously.[29] Briefly a known concentration of RNA (triplex or duplex) was kept in the sample and reference cells. Small aliquots of a known concentration of CHL were added into the sample cell and equal volume of the buffer was added to the reference cell. After each addition, solution was mixed and allowed to re-equilibrate for at least 5 minutes before recording the data. To avoid possible aggregation and prevent adsorption to the walls of the cuvette, the absorbance values have been kept at the minimum for optical studies. This spectrophotometric data were then cast into Scatchard plots of r/C_f *versus* r as described previously.[30]

Spectrofluorimetric studies

Steady state fluorescence measurements were performed on a Shimadzu RF-5301PC spectrofluorimeter (Shimadzu Corporation, Kyoto, Japan) which was attached to a highly sensitive temperature controller. Measurements were made in fluorescence free quartz cell of path length of 1 cm. A fixed concentration of CHL was titrated by increasing concentration of RNA triplex/duplex under constant stirring condition. All the measurements were conducted keeping an excitation and emission band pass of 3 and 5 nm respectively.

Analysis of binding data and evaluation of binding parameters

Binding data collected from spectrophotometric and spectrofluorimetric titration were used to construct Scatchard plots of r/C_f *versus* r.[31] Where r is the number of CHL moles bound per mole of triplex/duplex and C_f is the molar concentration of the free CHL. All Scatchard plots were nonlinear and showed negative slopes at low r values as observed in non-cooperative binding isotherms and therefore were analyzed by excluded site model for non-linear non-cooperative ligand binding phenomenon using McGhee and von Hippel equation, [32]

$$\frac{r}{C_f} = K'(1-nr)\left[\frac{(1-nr)}{\{1-(n-1)r\}}\right]^{(n-1)} \quad (1)$$

where, K' is the intrinsic binding constant to an isolated site, n is the neighbour exclusion parameter. The binding data were analyzed using the Origin 7.0 software to determine the best-fit parameters of K' and n.

Thermal Melting Experiments

Thermal melting of the triple and double helical forms of RNA in absence and in presence of the alkaloid was monitored by noting the change in UV absorption at 260 nm at different

temperatures using the same spectrophotometer. At each temperature the samples were allowed to equilibrate for sufficient time before noting the absorbance.

Determination of Binding Stoichiometry

To evaluate the binding stoichiometry of CHL with RNA triplex/duplex, Job's continuation method [33] was employed using the fluorescence spectroscopy. At constant temperature the fluorescence intensity (λ_{max}= 564 nm) was measured for the solution where concentrations of both triplex/duplex and CHL were varied but the sum of their concentrations kept constant at 10 μM. The relative difference of fluorescence intensity of CHL at 564 nm was plotted against the mole fraction of CHL. The break point of the plot gave the mole fraction of CHL in complex. The stoichiometry was obtained in terms of triplex/duplex:CHL $[(1-\chi_{CHL})/\chi_{CHL}]$ where χ_{CHL} denotes the mole fraction of CHL. The results reported are average of at least three experiments.

Mode of binding: fluorescence quenching studies

Fluorescence quenching studies were carried out with the anionic quencher potassium iodide. Solution of KI was mixed with the solutions of KCl in different proportions to give a fixed total ionic strength. Quenching experiments were performed at a constant [RNA-triplex or RNA-duplex]/[CHL] molar ratio monitoring fluorescence intensity changes at 564 nm as a function of the iodide concentration. The data were plotted in the form of Stern-Volmer equation[34]

$$\frac{F_o}{F} = 1 + K_{SV}[Q] \qquad (2)$$

Where, F_o and F are the fluorescence intensities of the alkaloid-complex with triplex or duplex (P/D=20) in the absence and in the presence of the quencher (Q) KI respectively and K_{SV} is the Stern-Volmer quenching constant. K_{SV} is indicative of the accessibility of the bulky quencher (iodide) to the fluorophore CHL. The slope of the F_o/F *versus* [KI] plot yields the value of K_{SV}.

Viscometric study

Viscometric measurements were carried out using a Cannon-Manning semi micro dilution viscometer type 75 (Cannon Instruments Co., State College, PA, USA) submerged vertically in a constant temperature bath maintained at 20±0.5 °C. Flow times of triplex and duplex RNA in absence and in presence of increasing concentration of CHL were measured in triplicate with an accuracy of ±0.01 s and the relative specific viscosity was calculated using the equation:

$$\frac{\eta'_{sp}}{\eta_{sp}} = \frac{[t_{complex} - t_0]}{[t_{control} - t_0]} \qquad (3)$$

Here, η'_{sp} and η_{sp} are the specific viscosity of triplex/duplex in presence and in absence of CHL respectively; $t_{complex}$ and $t_{control}$ are the time of flow of complex and control solution and t_o is the same for buffer solution as described previously.[35]

Sensitization of alkaloid emission, quantum efficiency determination and fluorescence energy transfer

Excitation spectrum of CHL was recorded in the wavelength range of 220-310 nm by monitoring the emission wavelength at 564 nm, to study the energy transfer from RNA triplex/duplex to CHL. This was confirmed further by recording of the nucleobase sensitized emission spectrum of CHL in the wavelength region 500-650 nm.[36] The quantum efficiency, Φ, of a ligand is a measure of amount of energy transfer from nucleic acid to ligand upon binding. Φ was calculated for different wavelengths from the ratio of the quantum efficiency of the ligand (CHL) bound to triplex/duplex (ϕ_b) to the quantum efficiency of free CHL (ϕ_f) using the equation [37]

$$\Phi = \frac{\phi_b}{\phi_f} = \frac{I_b}{I_f} \times \frac{\varepsilon_f}{\varepsilon_b} \qquad (4)$$

Where, I_b and I_f are the fluorescence intensities of bound and free CHL respectively. These values were obtained during fluorescence titration of CHL by U.A*U and A.U. ε_f is molar extinction value of free CHL which is already known. Calculation of determining ε_b value has been described by Garbett *et al.*[38] The ratio between the quantum efficiency of bound CHL excitation in the UV spectral region (Φ_λ) to that at 310 nm (Φ_{310}) was calculated. The wavelength 310 nm was chosen for the normalization process because of insignificant absorbance of U.A*U and A.U helices at this wavelength.

Circular dichorism spectral studies

Circular dichroism (CD) measurements were carried out on a PC-driven JASCO J815 spectropolarimeter (Jasco International Co., JAPAN) attached with a temperature controller and a thermal programmer model PFD-425L/15 interfaced in a rectangular quartz cuvette of 1 cm path length. All CD spectra were recorded in the wavelength range of 200–450 nm with a scan speed of 100 nm/min. Each spectrum was averaged from five readings. Final CD spectra were expressed in terms of molar ellipticity ([θ]) in units of deg cm^2 $dmol^{-1}$ by using the software provided with the spectropolarimeter. The molar ellipticity is based on RNA triplex/duplex concentration.

Isothermal titration calorimetry

Isothermal titration calorimetry (ITC) experiments were performed on a Microcal VP-ITC microcalorimeter (Microcal, Inc., Northampton, MA, USA) at 20 °C. The given origin 7.0 software was used for data interpretation. Aliquots of CHL(5 μL, 350 μM) in syringe was injected from a 299 μL rotating syringe rotating in 290 rpm to a isothermal chamber containing 1.4235 mL 25 μM of RNA triplex solutions. For the ITC experiment involving the duplex RNA, 7 μL of aliquot of CHL was injected from 250 μM solution to 25 μM solution of RNA duplex. The duration of each injection was 15 s and the delay time between the two injections were 300 s for CHL-triplex interaction study and the respective

durations were 15 s and 360 s for CHL-duplex interaction study. Each injection generated a heat burst curve with time. The area under each peak was integrated to get the corresponding heat of each injection by using origin 7.0 software. The calculated heat from control experiment was subtracted from the heat of CHL-RNA binding to get the actual heat of mixing. The heat of dilution was very negligible in this case. The resulting data were analyzed by using origin 7.0 software to obtain the value of binding constant (K_b), binding stoichiometry (N), enthalpy change (ΔH°) and free energy change (ΔG°) of binding interaction.

Results and discussion

Formation of U.A*U triple helix and characterization

U.A*U triplex was prepared by following the methods reported earlier.[39] In brief, equimolar solutions of poly(U) and A.U were mixed in SCH buffer and the mixture was heated up to 90 °C. The solution was kept at 90 °C for 45 minutes to complete the denaturation of the strands. Then the mixture was allowed to cool very slowly to reach a temperature of 10 °C and the mixture was kept in ice. Formation of the RNA triplex U.A*U was confirmed from CD and thermal melting studies. The CD spectra of the triplex and the corresponding duplex are shown in Fig. 2. In the Fig., curve 1 represents the triple helical form while curve 2 represents the corresponding double helical form of RNA. The CD spectrum of the triple helical form of RNA was characterized by a very strong positive peak at ~260 nm with molar ellipticity value ~ 23,000 deg cm^2 $dmol^{-1}$ and a negative peak at 241 nm with molar ellipticity value ~ 6,300 deg cm^2 $dmol^{-1}$. The characteristic CD spectrum of the triplex is markedly different from that of the duplex. In case of duplex positive peak was observed at 263 nm with molar ellipticity value ~27,400 deg cm^2 $dmol^{-1}$ and a negative peak was noted at 243 nm with molar ellipticity value ~9,300 deg cm^2 $dmol^{-1}$. Here CD data revealed that the spectra of both U.A*U triplex and A.U duplex showed a large positive band in the 250-

290 nm region and an weak negative band in the range 230-250 nm. In each case there is a small positive band below the 230 nm region. These are characteristics A-form structure of RNA. Therefore in both triple helical and double helical forms of RNA there is maintenance of A-form structure. It has been observed that there is lowering of ellipticity of all the three bands from duplex to triplex formation. Here the accommodation of the poly(U) strand in the groove of the A.U duplex to form the RNA triplex may cause the lowering of asymmetry in the overall molecule. Probably this is the reason for lower ellipticity value of the characteristics CD bands of U.A*U RNA triplex. Similar features of duplex and triplex forms of RNA have been reported.[39]

The melting profiles characterizing the RNA triplex is shown in the inset of Fig. 2. The profile shows biphasic transitions. Here the first transition at 35 °C indicates the displacement of the third strand from the triplex while the second transition around 46 °C represents the duplex denaturation to single strands. Thermal melting temperature (T_m) of the parent duplex was found to be around 45 °C. T_m data for the parent duplex and triplex RNA are in excellent agreement with the previous data [39] within experimental error. The biphasic melting of U.A*U triplex with the second transition temperature corresponding to that observed with their parent duplexes clearly indicates the formation and stability of the triplex.

UV-Visible absorption spectral studies of the interaction

Binding of CHL with triple and double helical forms of RNA was first monitored by absorption spectral measurements. Absorption spectral studies were carried out in SCH buffer at 20 °C. In presence of both triplex and duplex RNA the spectrum of the alkaloid was perturbed. With increase in the concentration of RNA triplex/duplex, absorption peak of CHL at 316 nm was red shifted and a hypochromic shift was observed (Representative spectra Fig. 3A and 3B). Such finding can be explained as follows: the empty π^*-orbital of

the ligand molecule couples with the π^*-orbital of the RNA bases causing an energy decrease and a decrease of the π–π^* transition energy. As a result a bathochromic shift is noted. Again, the empty π^*-orbital is partially filled with electrons to reduce the transition probability which causes hypochromism.[40] Three clean isosbestic points were observed in each case. Appearance of such sharp isosbestic points indicated the presence of two state systems consisting of bound and free alkaloid species enabling application of equilibrium conditions in the complexation. Optical properties of free and RNA bound CHL are presented in Table S1. Spectra of free and bound alkaloid in presence of excess triple and double helical forms of RNA are shown in Fig. 3. The data obtained from reverse spectrophotometric titration (described earlier in methods) were cast into the form of Scatchard plot of r/C_f *versus* r (Fig. 4). It was found that the plot was nonlinear and there was always negative slope in all r values. Such negative value of slope for whole range of r indicated non-cooperative type of association of CHL with both triple and double helical form of the RNA. In this case it is to be noted that we could not reach very low value of r when we used the direct titration of CHL with increasing amount of the polymer. The Scatchard plots were fitted and analyzed by non-cooperative binding using McGhee-von Hippel equation.[32] The binding constants for the association of CHL with U.A*U and A.U were 30.2×10^5 M^{-1} and 3.6×10^5 M^{-1} respectively and the respective binding stoichiometries were ~4.3 and 3.8. Binding parameters are presented in Table 1. Our data indicate that the alkaloid binds more strongly with triple helical form of RNA compared to that of the parent duplex form. The strong binding of CHL to RNA triplexes in comparison to the RNA duplex can be explained in terms of an effective stacking and relief of electrostatic expulsion among the three strands of the triplex leading to a favorable orientation at the intercalation site. Similar kind of observation has been reported for sanguinarine,[19] berberine,[19] and also for aristololactam-β-D-glucoside.[39] Scarcia & Shafer (1991) also

showed that binding constant of ethidium bromide-triplex DNA association is higher than the corresponding duplex complex.[41] A reverse effect has also been reported in case of ethidium bromide-RNA triplex interaction.[42] Recently Bhowmik *et al* (2014) have shown higher binding affinity of some berberine analogs with DNA triplex than the parent duplex form.[43]

Fluorescence spectral studies of the interaction

Fluorescence spectroscopy is another useful technique for the study of the interaction of ligand with nucleic acid. Binding of CHL with triple and double helical forms of RNA was further investigated by fluorescence intensity measurements. Fluorescence titrations of CHL with U.A*U and A.U were carried out at 20 °C in SCH buffer. The emission spectrum of CHL was recorded in the wavelength range 470-750 nm by exciting at 400 nm. The excitation and emission slits were 3 and 5 nm respectively. This excitation wavelength was chosen since at this wavelength the alkanolamine form of the alkaloid has no absorption.[25]CHL is a non fluorescent molecule. On addition of either forms of RNA to CHL fluorescence intensity of CHL was enhanced gradually (Fig. S1). The enhancement was more in case of triplex bound CHL than duplex bound CHL. A blue shift of emission peak of CHL was observed in presence of both forms of RNA. The data were cast into form of Scatchard plot . The plots showed negative slope at low *r* values indicating non-cooperative type of binding. The binding constants calculated from the fluorescence data as per the Scatchard plot and the non-cooperative binding model of McGhee-von Hippel analysis are given in Table 1. The values are in excellent agreement with the spectrophotometric results (Table 1). Comparative studies of binding of triplex and duplex with CHL manifested the preferential binding of CHL with triplex than with the duplex.

Thermal Melting Study

Thermal melting profiles of the U.A*U triplex in absence and in presence of CHL are presented in Fig. 5A. CHL strongly stabilizes the third strand of the triplex compared to the respective Watson and Crick duplex. Thermal melting data are presented in Table 2. Studies with the corresponding parent duplex also indicate that CHL enhances the T_m of the parent duplex (Fig. 5B). On binding with CHL third strand of triplex is stabilized up to 18.5 °C and Watson–Crick strand is stabilized up to 7.5 °C. Whereas duplex A.U is stabilized up to 8 °C due to binding interaction with CHL. Such thermal stabilization of the third strand of U.A*U triplex by another benzophenanthridine alkaloid sanguinarine has been reported by Das *et al.*[19] Sinha *et al* have shown the thermal stabilization of the third strand of U.A*U by the DNA binding compounds berberine, palmatine and coralyne.[44] These compounds have been shown to have very small stabilizing effects on the double stranded form of RNA compared to the third strand.

From the melting experiment it is clear that CHL stabilizes the Hoogsteen base paired third strand by significantly greater extent compared to the Watson Crick base paired strand. Our data suggest that the effective stacking arrangement between the alkaloid and the third strand may play an important role in the triplex stability as the template duplex is comparably less stabilized by the alkaloid under identical conditions.

Binding stoichiometry (Job's plot)

The binding stoichiometry and the possible number of binding sites of CHL on triple and double helical forms were determined by continuous variation analysis (Job's plot) in fluorescence. The plot (Fig. 6) revealed a single binding mode for the association of the alkaloid on either triplex or duplex RNA. The intersection points were observed at χ_{CHL}=0.21 and 0.23 for CHL-triplex and CHL-duplex complexation respectively. The stoichiometry was found to be ~3.8 and 3.3 for the complaxation of CHL with triple and

double helical form of RNA. This data is in accordance with the data obtained from the analysis of Scatchard plot. Lower stoichiometry of binding indicates closer binding sites of CHL-triplex/duplex RNA as well as stronger association with RNA.[44]

Mode of binding: Fluorescence quenching studies

Fluorescence quenching experiment is a useful method to address the mode of interaction of small molecules to different polymorphic forms of nucleic acids.[34] In fact, molecules that are either free or bound on the surface of nucleic acid are easily accessible for the quencher. But those molecules which are inserted between the bases of polynucleotide are not accessible to the quencher. Negative charge on the phosphate backbone of the double or triple helical form of nucleic acid causes an electrostatic barrier on the helix surface and restricts the penetration of an anionic quencher into the interior core of the helix. As a result very little or no quenching may be observed in the presence of such quencher if the binding involves strong stacking or intercalation. Therefore the magnitude of the Stern-Volmer quenching constant (K_{SV}) of the ligands that are bound inside will be lower than that of the free ligand. It is observed that binding to the triple and double helical forms of RNA resulted in an increase of the fluorescence intensity of CHL. Representative Stern-Volmer plots for free, U.A*U and A.U bound CHL are shown in Fig. 7. Stern Volmer constants were 12.8, 4.9, 8.1 M^{-1} for free, triplex bound and duplex bound CHL respectively. K_{SV} values indicated that bound CHL was less accessible to the quencher or in other words were considerably protected and sequestered away from the solvent suggesting intercalative binding with both triple and double helical forms of the RNA. Our data revealed that the accessibility of the quencher to CHL was less when it was bound to triple helical RNA compared to the double helical form. In other words the alkaloid may have better intercalation penetration in the triple helical form of RNA compared to that in double stranded form.

Viscometric study

The mode of binding of CHL with triple and double helical forms of RNA was subsequently confirmed to be intercalative from viscosity studies also. Intercalative mode of binding of molecules between DNA bases is known to increase the viscosity of the solution owing to unwinding and elongation of the double helix as proposed by Lerman.[45] This is due to the fact that intercalation leads to enhancement of the axial length of the nucleic acid resulting in more rigidity due to enhancement of the frictional coefficient. The binding mode of CHL to the RNA triplex and duplex was probed by measuring the viscosity of the triplex/duplex solution in the presence of increasing concentrations of the alkaloid. The effect of CHL binding on the viscosity of triplex and duplex RNA solution is represented in Fig. 8. The relative specific viscosity of the RNA-alkaloid complex increased with increase in D/P ([CHL]/[Triplex or duplex]). Our results clearly underscore the intercalation mode of binding of CHL to both U.A*U and A.U. This data along with the hypochromism in the absorbance spectrum and fluorescence quenching results support an intercalating complexation of CHL with both triple and double helical RNA.

Energy transfer and quantum yield

Interaction of CHL with U.A*U and A.U was evidenced from spectrophotometric and spectrofluorimetric studies along with fluorescence quenching and thermal melting experiments. Fluorescence quenching and viscometric studies indicate the intercalative mode of binding of the alkaloid with both triplex and duplex forms of RNA. Stern Volmer constant data revealed that the intercalation geometry is more favoured in case of triplex RNA compared to the duplex one. The binding of CHL to RNA triple and double helices was exploited to study the excited state energy transfer from RNA bases to bound CHL molecules. Energy transfer phenomenon was studied by recording the excitation spectra (Fig. S2) of CHL in presence of triplex and duplex RNA (concentration ratio of

CHL:triplex/duplex=1:25). Excitation spectra of triplex and duplex bound CHL were monitored in the wavelength range 220-510 nm by fixing the fluorescence emission wavelength at 564 nm. In absence of triplex the observed excitation spectrum of CHL (inset of Fig. S2, spectra 1) exactly matches with the absorption spectrum of CHL (inset of Fig. S2, spectra 2) in the wavelength range 300-500nm. But in this case there was absence of strong peak around the wavelength range 260-280 nm in the excitation spectrum of CHL whereas in absorption spectrum of CHL a strong peak is appeared. From the obtained result we can say that the emission of CHL at 564 nm might not be due to the absorption around 260-280 nm. This observation was further accomplished from the emission spectrum of free CHL when it is excited at 270 nm. No significant emission was observed in the wavelength range 300-550 nm. A peak around 266 nm was seen in the excitation spectrum of triplex bound CHL but such peak was absent in case of free CHL and for free triplex (Fig. S2). The ratio of excitation spectra of CHL bound triplex is represented in Fig. 9A. This plot indicates direct emission from CHL and the ratio greater than unity indicates sensitization by RNA triplex. Appearance of very strong excitation band around 270 nm in the bound complex can only be explained on the basis of absorption of energy and then its transfer by the RNA bases to the alkaloid. Absence of any band in the excitation spectrum of RNA triplex in the wavelength region 220-300 nm, when emission was monitored at 564 nm, is consistent with the interpretation of energy transfer from RNA base triplets to CHL. Energy transfer from RNA triplex to CHL was further established by sensitized emission spectra (Fig. 9B). Fluorescence energy transfer was also confirmed from the plot of relative quantum yield *versus* wavelength. A plot of Φ_λ/Φ_{310} against wavelength at a P/D (RNA base triplet/CHL molar ratio) of 25 is shown in Fig. 9C. An increase in quantum efficiency in the RNA absorption region was observed. This implies energy transfer from the RNA bases to bound alkaloid molecules and also indicates intercalative mode of binding.

In case of binding of CHL with the double helical form of the RNA we got similar observation as that of CHL-triplex complexation, though the extent of changes was less (data not shown). From our experimental data it is clear that there occurs energy transfer from both triplex and duplex RNA to the alkaloid moiety. Representative scheme for energy transfer is shown in the Fig. 9D. Such fluorescence energy transfer has been reported in case of CHL-DNA binding[25] and CHL-poly (A) binding.[28] Thus from the present study it can be concluded that both DNA as well as RNA base doublet and triplet can transfer energy to CHL when the alkaloid is intercalated in the DNA/RNA structure.

Circular Dichroism Study

The effect of CHL on the CD spectrum of triple and double helical forms of the RNA is represented in Fig. 10. In presence of the alkaloid, the CD spectrum of U.A*U triplex was perturbed (Fig. 10A). There was a red shift of the 260 nm band followed by concomitant increase of the ellipticity from ~21,000 to ~26,000 deg cm^2 $dmol^{-1}$. Two clear isoelliptic points were observed at 235 and 260 nm in the series of spectra. The binding of CHL to the triple helix was further characterized by the appearance of extrinsic CD band in the 310-370 nm region. Similar kind of observations have been reported for other DNA binding agents.[19,25,44] Binding of CHL to the A·U duplex (Fig. 10B) causes comparatively less perturbation in the CD spectrum. Here also there is appearance of positive extrinsic CD around 330 nm. In this case only one isoelliptic point at 335 nm was noted. The appearance of induced CD band in the region of 300-375 nm clearly indicates the binding of CHL in the asymmetric environment of RNA triplex/duplex.

Isothermal titration calorimetry (ITC)

ITC is an effective tool for thermodynamic characterization of binding of small molecules to macromolecules.[46] Fig. 11 represents the raw data resulting from the injection of CHL into the RNA triplex/duplex solution. Each of the heat burst curve in the Fig. 11 represents a

single injection. The corresponding area under each heat burst curve is integrated to calculate the associated heat change. Corrections were done by subtracting the dilution heat from the each injection heats. Dilution heats were derived by injecting the same amount CHL into the working buffer. In the lower panels of Fig. 11, the resulting corrected heat is plotted against the respective D/P (CHL/RNA molar ratio) values. Here data points reflect the experimental injection heats while the solid lines reflect calculated fits of data. The binding nature is exothermic in nature in case of both CHL-U.A*U (Fig. 11A, lower panel) and CHL-A.U (Fig. 11 B, lower panel) interaction. Calorimetric data were fitted to a single set of identical sites that resulted a good fitting of the experimental data. The calculated binding constants, number of occluded sites, enthalpy and entropy of binding are presented in Table 3. ITC data presents valuable thermodynamic data regarding the actual mode of binding of the alkaloid with two different forms of RNA. The binding affinity of CHL was found to be one order higher for triplex when compared with the duplex RNA. The strong binding of CHL to RNA triplex in comparison to the duplex can be explained in terms of an effective stacking and relief of electrostatic expulsion among the three strands of the triplex leading to a favorable orientation at the intercalation site. Binding parameters obtained from ITC experiments are in excellent agreement with the data obtained from spectrophotometric and spectrofluorimetric measurements (Table 1). The binding of CHL with both triple helical and double helical forms of the RNA was favoured by both negative enthalpy change and positive entropy change. Here, in both the cases, negative enthalpy and positive entropy changes compensate each other to produce a negative free energy change. Conceptually, the contribution to the thermodynamic parameters for the binding process of small molecules with nucleic acid structure is divided into the following parts. (i) Contributions from hydrophobic part and hydrogen bonding due to molecular interactions between the bound ligand and nucleic acid binding site, (ii) contributions due to

conformational changes in either the ligand or the nucleic acid upon binding, (iii) contributions from coupled processes like ion release and proton transfer, (iv) changes in the water of hydration and (v) a contribution from increase in phosphate spacing that results from intercalation-induced conformational changes in the nucleic acid. Positive entropy change values indicate displacement of counter ions, disruption of water molecules from the hydration shell of RNA and stronger association. It also suggests that the hydrophobicity of the compound is playing an important role in the transfer of the CHL molecules from solvent to intercalation site. It has been proposed by Breslauer and coworkers that such solvent induced positive entropy contributions may be a general feature of the thermodynamic forces that drive ligand-DNA interactions.[47] Thus, the variation in enthalpy and entropy changes for CHL-triplex and CHL-duplex RNA interaction presented in Table 3 may be correlated with the differences in the hydration properties (perhaps conformation) of triplex and duplex structures. Less positive entropy change contribution in case of CHL-triplex RNA complexation may be attributed to the more ordered structure of RNA triplex compared to the duplex one.

Conclusion

The present study reveals that CHL exhibits stronger binding with RNA triplex than to respective parent duplex and the alkaloid stabilizes more effectively the Hoogsteen base paired third strand of U.A*U compared to their respective Watson-Crick strand. Viscometric data along fluorescence quenching results revealed that the mode of binding of CHL to both triple and double helical forms of the RNA was intercalation. From sensitized fluorescence experiment it is suggested that there was energy transfer from RNA base triplets and doublets to CHL which in turn corroborated intercalative mode of binding of CHL to either form of the RNA. The process of binding of CHL to triplex and duplex forms of RNA was favoured by both negative enthalpy and positive entropy changes. The results

presented here may be useful for formulating effective antigene strategies involving benzophenanthridine alkaloids and the RNA triplex.

Acknowledgement

LH and ABP thank to the University Grant Commission, Government of India, for the award of Junior research Fellowship and Senior Research Fellowship respectively. SB thanks the University Grant Commission, Government of India, for the award of RGNF research Fellowship.

References

1 G. Felsenfeld, D. R. Davies and A. Rich, *J. Am. Chem. Soc.,* 1957, **79**, 2023–2024.

2 A. Jain, A. Bacolla, P. Chakraborty, F. Grosse and K. M. Vasquez, *Biochemistry,* 2010, **49**, 6992-6999.

3 J. S. Mattick, R. J. Taft and G. J. Faulkner, *Trends Genet*., 2010, **26**, 21-28.

4 L. Tan, L. Xie, X. Sun, L. Zeng and G. Yan, *J. Inorg. Biochem.*, 2013, **120**, 32-38.

5 F. A. Buske, J. S. Mattick and T. L. Bailey, *RNA Biol*., 2011, **8,** 427–439.

6 H. Torigoe, O. Nakagawa, T. Imanishi, S. Obika and K. Sasaki, *Biochimie*, 2012, **94**, 1032-1040.

7 F. Svinarchuk, J. Paoletti and C. Malvy, *J. Biol. Chem.,* 1995, **270**, 14068-14071.

8 K. R. Fox and T. Brown, *Biochem. Soc. Trans*., 2011, **39**, 629–634.

9 D. Bhowmik, S. Das, M. Hossain, L. Haq and G. S. Kumar, *PLoS One*, 2012, **7**, e37939.

10 D. Bhowmik, F. Buzzetti, G. Fiorillo, P. Lombardi and G. S. Kumar, *Spectrochimica Acta Part A*, 2014, **120**, 257–264.

11 A. Beck, V. Vijayanathan, T. Thomas and T. J. Thomas, *Biochimie*, 2013, **95**, 1310-1318.

12 F. Riechert-Krause, K. Autenrieth, A. Eick and K. Weisz*, Biochemistry*, 2013, **52**, 41-52.

13 S. Basili, A. Bergen, F. Dall'Acqua, A. Faccio, A. Granzhan, H. Ihmels, S. Moro and G. Viola, *Biochemistry*, 2007, **46**, 12721-12736.

14 S. Nafisi, Z. M. Malekabady,and M. A. Khalilzadeh, *DNA & Cell Biology,* 2010, **29,** 753-761.

15 M. Stiborova, V. Simanek, E. Freic, P. Hobzad and J. Ulrichova, *Chem.biol. interact.,* 2002, **140**, 231-242.

16 H. Bochorakov, H. Paulov, P. Musil and E. Taborsk, *J. Pharm. Biomed. Anal.,* 2007, **44**, 283–287.

17 P. Giri and G. S. Kumar, *Biochim. Biophys. Acta*, 2007, **1770**, 1419–1426.

18 M. Maiti and G. S. Kumar, *J. Nucl. Acids*, 2009, **2010**, 1–24.

19 S. Das, G. S. Kumar, A. Ray and M. Maiti, *J.Biomol. Struct. Dyn.,* 2003*,* **20**, 703-712.

20 A. Cabrespine, J. O. Bay, C. Barthomeuf, H. Cure, P. Chollet and E. Debiton, *Anticancer Drugs,* 2005, **16,** 417-422.

21 S. J. Chmura, M. E. Dolan, A. Cha, H. J. Mauceri, D. W. Kufe and R. R. Weichselbaum, *Clin. Cancer Res.,* 2012, **6,** 737-742.

22 S. Yamamoto, K. Seta, C. Morisco, S. F. Vatner and J. Sadoshima, *J. Mol. Cel. Cardiol.,* 2001, **33,** 1829-1848.

23 Z. F. Zhang, Y. Guo, J. B. Zhang and X. H. Wei, *Arch. Pharm. Res.,* 2011, **34,** 791-800.

24 J. O'Neill, M. Manion, P. Schwartz and D. M. Hockenbery, *Biochim. Biophys. Acta,* 2004, **1705,** 43-51.

25 P. Basu, D. Bhowmik and G. S. Kumar, *J. Photochem. Photobiol. B,* 2013, **129,** 57-68.

26 L. P. Bai, Z. Z. Zhao, Z. Cai and Z. H. Jiang, *Bioorg. Med. Chem.,* 2006, **14,** 5439-5445.

27 J. Li, B. Li, Y. Wua, S. Shuang, C. Dong and M. M. F. Choi, *Spectrochim. Acta. Part A,* 2012, **95,** 80–85.

28 A. B. Pradhan, L. Haque, S. Bhuiya and S. Das, *RSC Adv.,* 2014**, 4**, 52815-52824.

29 N. K. Lee, A. Johner, IL. B. Lee, and S.C. Hong, Eur. Phys. J. E., 2013, **36**, 13057-13064.

30 S. Das, G. S. Kumar and M. Maiti, *Biophysical Chemistry,* 1999, **76**, 199–218.

31 G. Scatchard, *Ann. N Y Acad Sci.,* 1949, **51**, 660–762.

32 J. D. McGhee and P. H. von Hippel, *J Mol. Biol.,* 1974, **86**, 469–489.

33 P. Job, *Annali di Chimica Applicata,* 1928, **9**, 113-203.

34 J. R. Lakowicz, *Principles of Fluorescence Spectroscopy*; Plenum Press: New York, U.S.A., 2006.

35 A. B. Pradhan, L. Haque, S. Roy and S. Das, *PLoS One*, 2014, **7**, e87992.

36 C. V. Kumar, E. H. A. Punzalan and W. B. Tan, *Tetrahedron,* 2000, **56**, 7027-7040.

37 J. B. LePecq and C. Paoletti, *J Mol. Biol.,* 1967**, 27**, 87–106.

38 N. C. Garbett, N. B. Hammond, D. E. Graves, *Biophysical J.,* 2004, **87**, 3974–3981.

39 A. Ray, G. S. Kumar, S. Das and M. Maiti, *Biochemistry,* 1999**, 38***,* 6239-6247.

40 G. Zhang, J. Guo, J. Pan, X. Chen and J. Wang, *J. Mol. Struct.***,** 2009, **923,** 114-119.

41 P. V. Scaria and R. H. Shafer, *J. Biol. Chem.,* 1991, **266**, 5417-5423.

42 B. Garcia, J. M. Leal, V. Paiotta, S. Ibeas, R. Ruiz, F. Secco and M. Ventturini, *J. Phys. Chem. B*, 2006, **110**, 16131-16138.

43 D. Bhowmik and G. S. Kumar*, Mol. Biol. Rep.,* 2013, **40**, 5439–5450.

44 R. Sinha and G. S. Kumar, *J. Phys. Chem. B*, 2009, **113**, 13410-13420.

45 L. S. Lerman, *J. Mol. Biol.,* 1961, **3,** 18-30.

46 S. Das and G. S. Kumar, *J. Mol. Struct.*, 2008, **872**, 56–63.

47 T. V. Chalikian, G. E. Plum, A. P. Sarvazyan and K. J. Breslauer, *Biochemistry* 1994, **33**, 8629 -8640.

Fig. legend

Fig. 1 Chemical structure of CHL.

Fig. 2 Characteristic circular dichroic spectra of U.A*U triplex (30.2 μM, Curve1) and A.U duplex (30.2 μM, Curve 2) in SCH buffer at 20 °C. Inset: Thermal melting profiles of U.A*U triplex (20.1 μM, -●-) and A.U duplex (20.1 μM, -●-) in SCH buffer.

Fig. 3 Absorption spectra of free CHL (2.73 μM, curve 1, panel A and B) and bound CHL in presence of saturating concentrations of U.A*U triplex (curve 2, panel A) and A.U duplex (curve 2, panel B) in SCH buffer at 20 °C.

Fig. 4 Scatchard plot for the binding of CHL to U.A*U triplex (panel A) and A.U duplex (panel B). The solid line is the non linear least squares best fit of the experimental points to the Von-Hippel equation.

Fig. 5 Thermal melting profiles of U.A*U triplex (panel A) and A.U duplex (panel B) in absence and in presence of CHL. (A) 18.0 μM U.A*U triplex (-●-) and its complexation CHL at D/P of 0.025 (-●-), 0.05 (-●-), 0.10 (-●-) and 0.25 (-●-); (B) 18.0 μM A.U duplex (-●-) and its complexation CHL at D/P of 0.05 (-●-), and 0.25 (-●-) in SCH buffer.

Fig. 6 Continuous variation plot for the binding of CHL with U.A*U triplex (panel A) and A.U duplex (panel B) in SCH buffer at 20 °C. The relative difference in fluorescence intensity at 564 nm was plotted against the mole fraction of CHL added.

Fig. 7 Stern-Volmer plots for the quenching of CHL fluorescence by KI in the absence (●) and in presence of U.A*U triplex (●) and A.U duplex (●) in SCH buffer at 20 °C.

Fig. 8 A plot of change of relative specific viscosity of U.A*U triplex (●) and duplex (●) with increasing concentration of CHL in SCH buffer at 20 °C. The concentrations of triplex and duplex were 300 μM.

Fig. 9 (A) Fluorescence excitation spectrum of CHL recorded in presence of U.A*U triplex at emission of wavelength at 564 nm. (B) Sensitized fluorescence spectra of CHL in presence (curve 1) and in absence of U.A*U triplex (curve 2). (C) Variation of relative quantum yield of CHL in the presence of U.A*U triplex. (D) Energy transfer scheme

illustrating the sensitization of alkaloid emission by the RNA triplex bases. All the spectra were taken in SCH buffer at 20 °C.

Fig. 10 (A) Circular dichroic spectra of U.A*U triplex (25.3 μM) treated with varying concentrations of CHL in SCH buffer at 20 °C. (A) Curves 1-6 represent the CHL concentrations of 0, 2.5, 5.1, 6.8, 8.5 and 10.1 μM respectively. (B) Circular dichroic spectra of duplex (25.0 μM) with varying concentrations of CHL in SCH buffer at 20 °C. The curves 1–5 represent the CHL concentrations of 0, 2.5, 5.1, 6.8 and 10.5 μM respectively.

Fig. 11 ITC profile for the binding of CHL to U.A*U triplex (panel A) and A.U duplex (panel B) in SCH buffer at 20 °C. The upper panels represent the raw data for the sequential injection of the CHL into the U.A*U triplex (panel A, curves on the bottom) and A.U duplex (panel B, curves on the bottom) solutions respectively and CHL dilution control (curves on the top off set for clarity). The lower panels show the corresponding normalized heat signals versus molar ratio. The data (closed circles) were fitted to a one site model and the solid lines represent the best fit data.

Table 1

Binding parameters for the interaction of CHL with Triplex and duplex in SCH buffer at 20 °C obtained from spectrophotometry and spectrofluorimetry.[a]

Parameters	Methods	Triplex	Duplex
K′ (x10^5 M^{-1}), the intrinsic binding constant	[A] Spectrophotometry	30.2	3.6
	[B] Spectrofluorimetry	30.5	3.3
n, the no of base excluded	[A] Spectrophotometry	4.3	3.8
	[B] Spectrofluorimetry	4.1	3.9
K_{SV}, the Stern Volmer quenching constant (L mol^{-1})	Spectrofluorimetry	Free: 12.8 Bound: 4.9	Free: 12.8 Bound: 8.1
Stoichiometry from Job's plot	Spectrofluorimetry	3.8	3.3

[a] Average of three determinations

Table 2

Effect of CHL on the thermal stability of RNA triplex and duplex

RNA/Complex	D/P	T_m(°C) 3→2	T_m(°C) 2→1	ΔT_m(°C) 3→2	ΔT_m(°C) 2→1
U.A*U	0	35	46		
U.A*U+CHL	0.025	37	47.5	2.0	1.5
	0.050	39.5	49.0	4.5	3.0
	0.100	50.0	50.0	15.0	4.0
	0.250	53.5	53.5	18.5	7.5
A.U	0		45.0		
A.U+CHL	0.05		48.0		3.0
	0.25		53.0		8.0

Table 3

Thermodynamic parameters for the interaction of CHL with U.A*U triplex and A.U duplex from ITC experiments.

Polymer	K´(x10^5 M^{-1})	N	n	$\Delta G°_{293K}$ (kcal.mol^{-1})	$\Delta H°$ (kcal. mol^{-1})	$T\Delta S°$ (kcal.mol^{-1})
Triplex (U.A*U)	28.9	0.26	3.8	-8.66	-5.75	2.92
Duplex (A.U)	3.5	0.30	3.3	-7.43	-4.07	3.36

Graphical Abstract

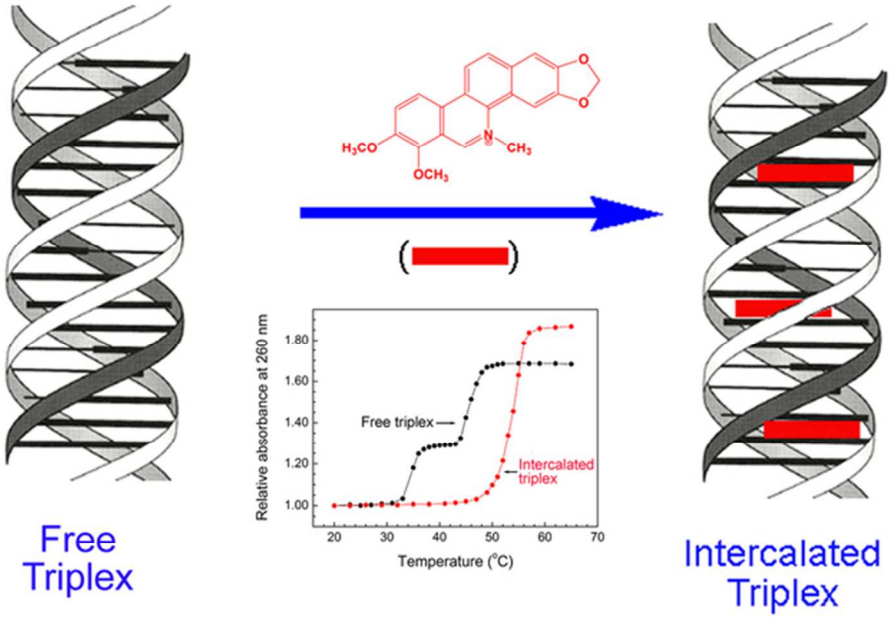

59x46mm (300 x 300 DPI)

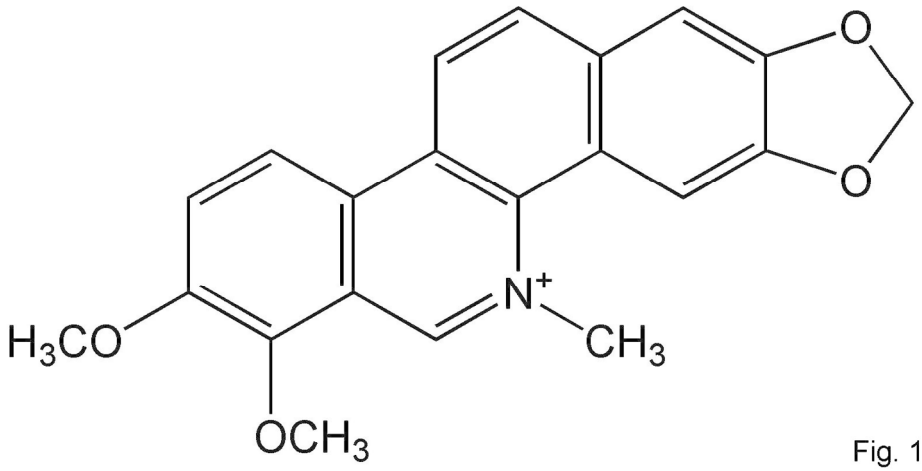

Fig. 1

146x76mm (300 x 300 DPI)

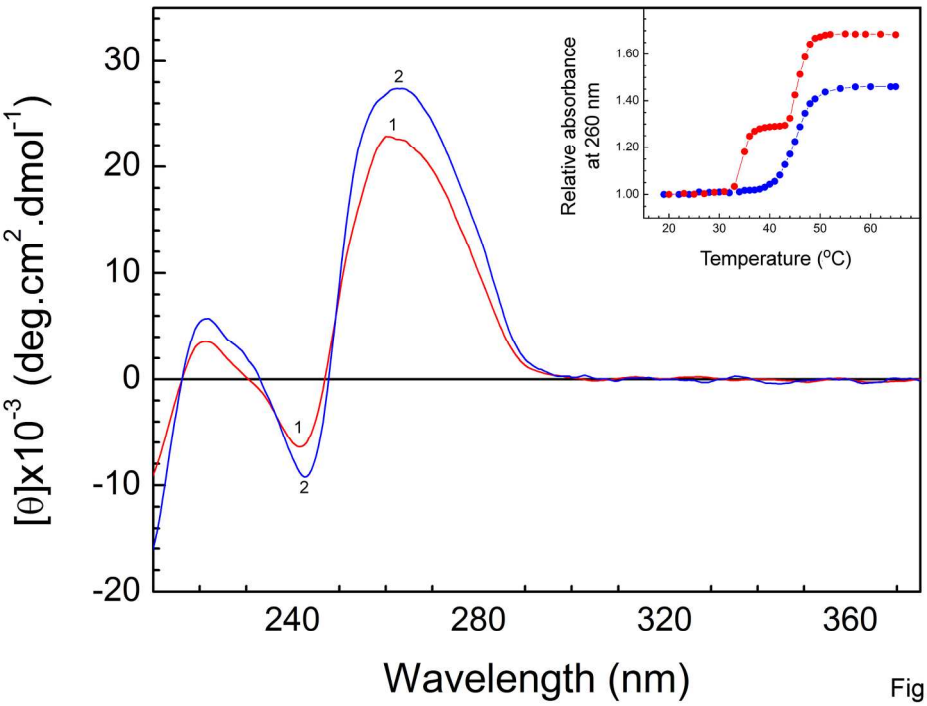

Fig. 2

193x149mm (300 x 300 DPI)

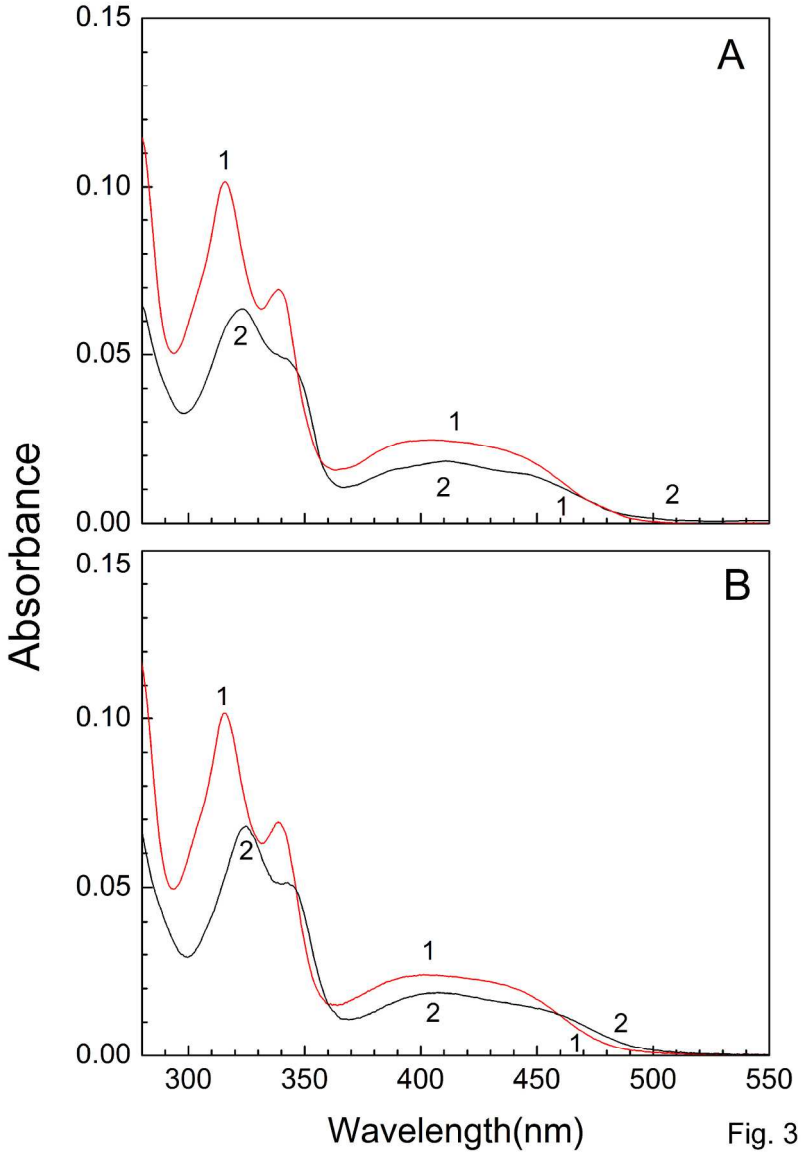

Fig. 3

180x256mm (300 x 300 DPI)

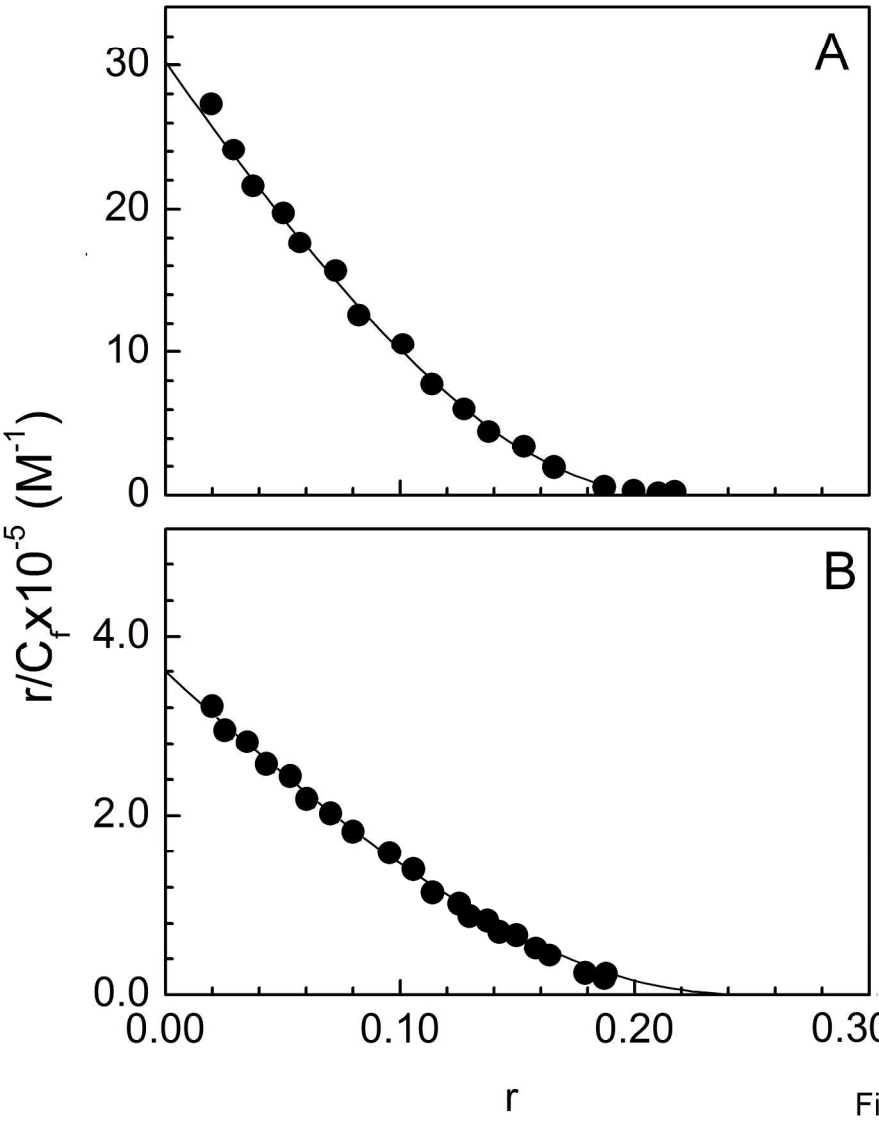

Fig. 4

244x295mm (300 x 300 DPI)

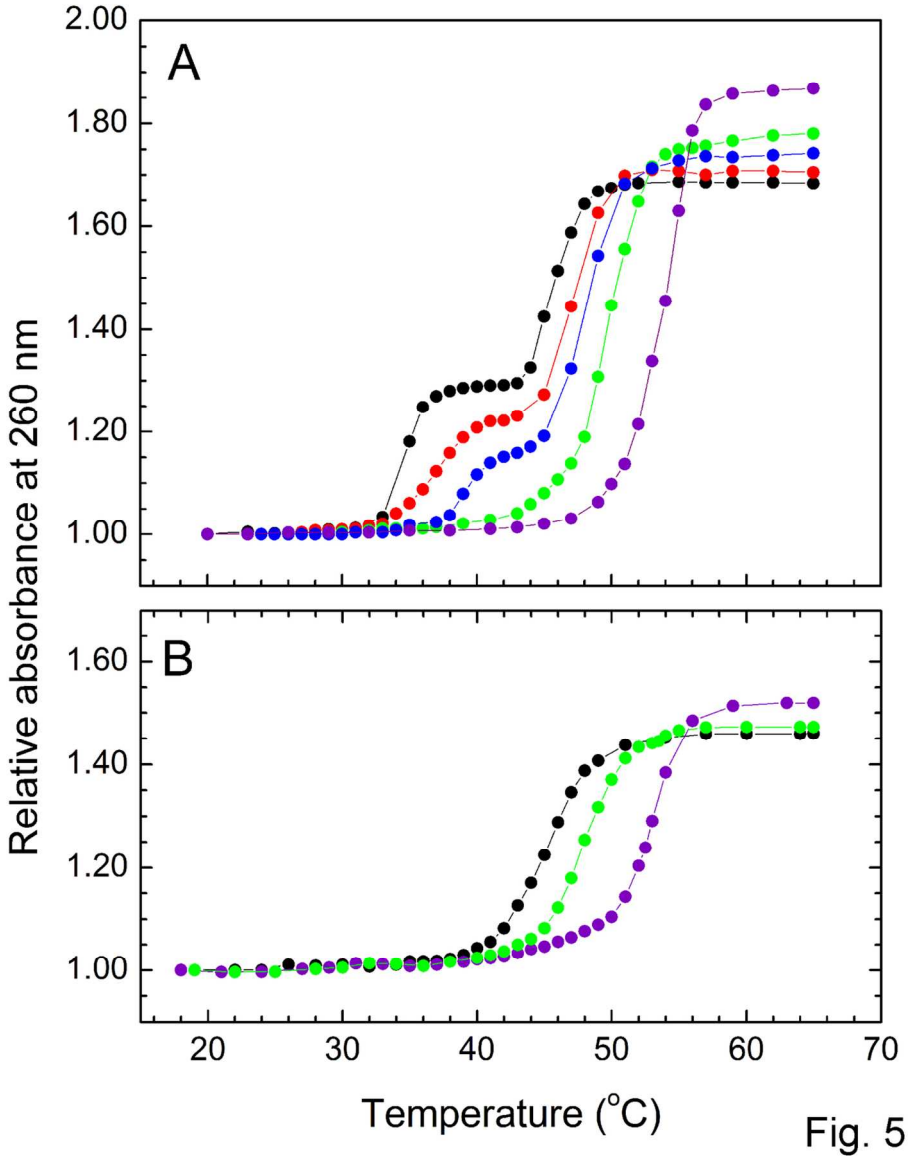

Fig. 5

124x152mm (300 x 300 DPI)

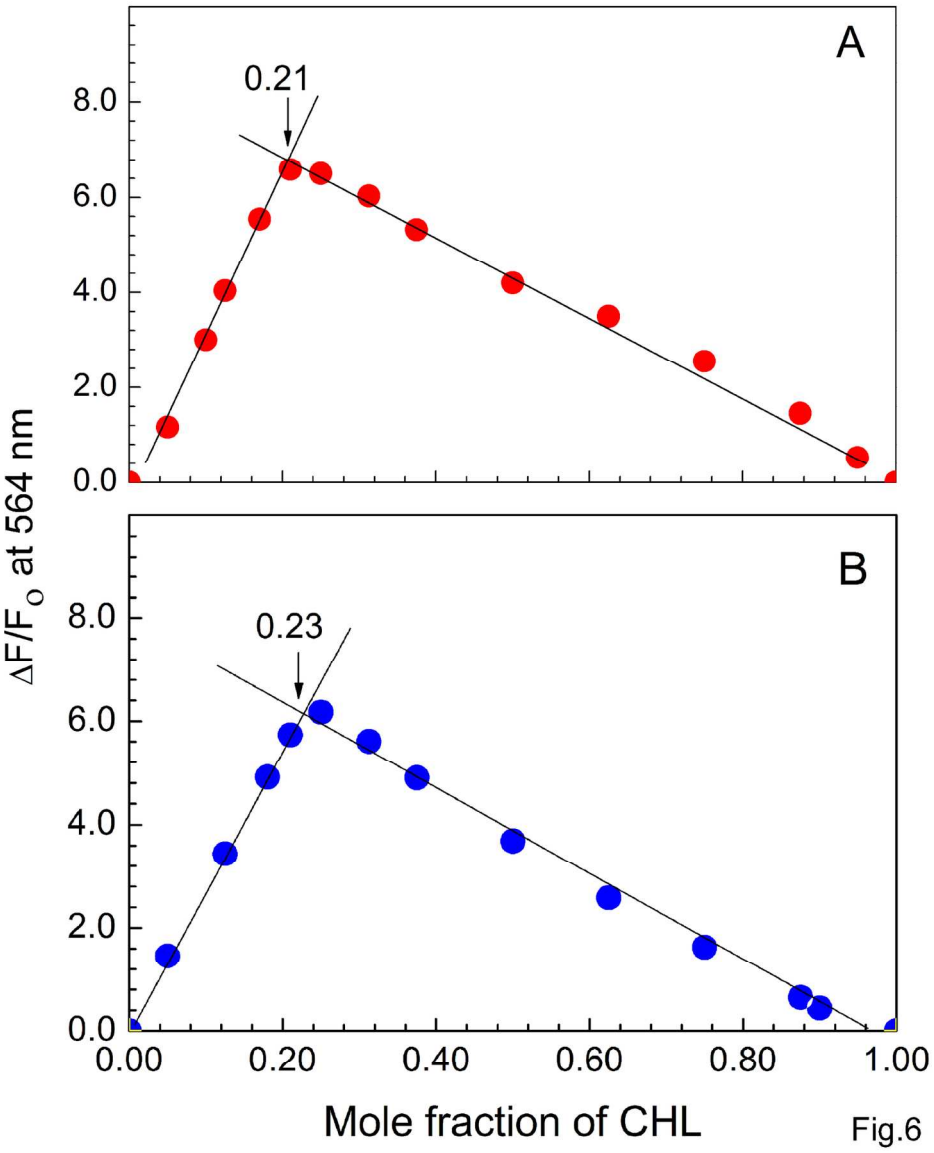

Fig.6

152x183mm (300 x 300 DPI)

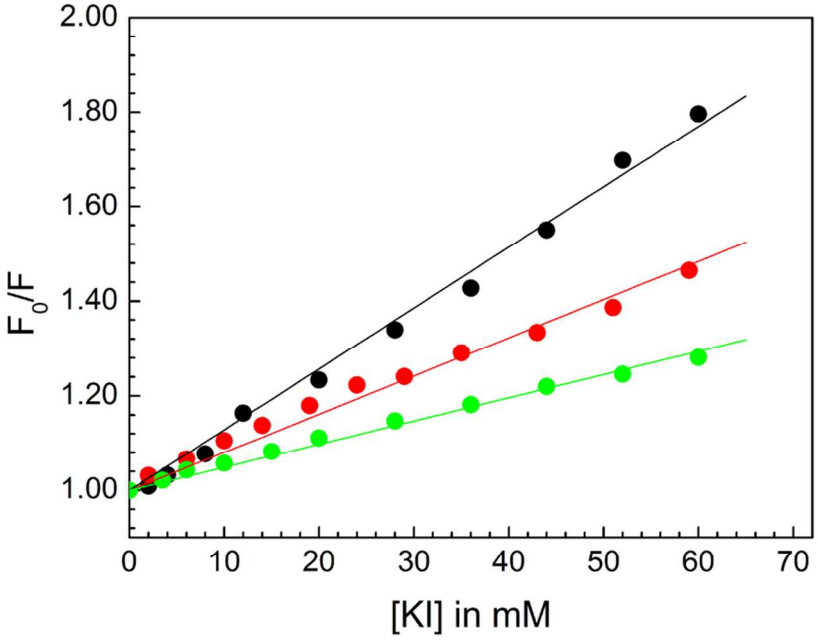

Fig. 7

92x66mm (300 x 300 DPI)

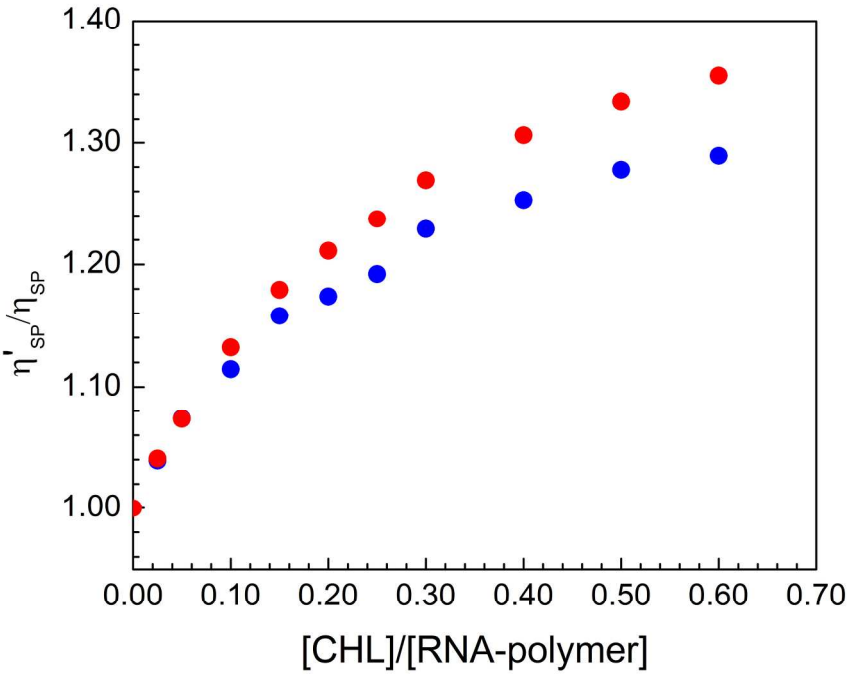

Fig. 8

208x159mm (300 x 300 DPI)

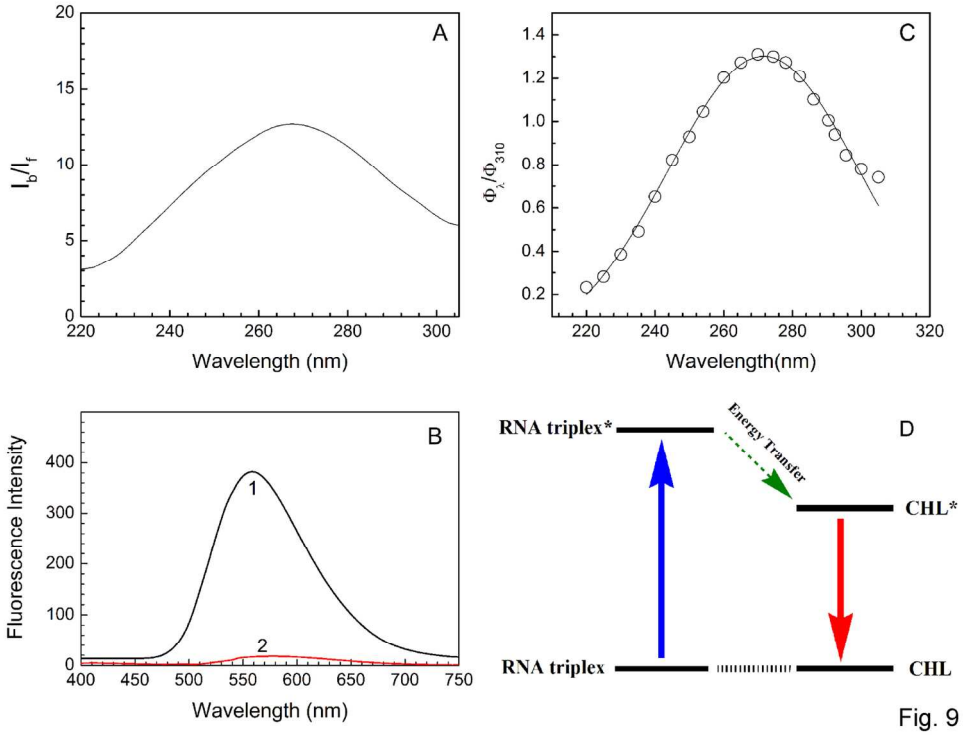

Fig. 9

154x117mm (300 x 300 DPI)

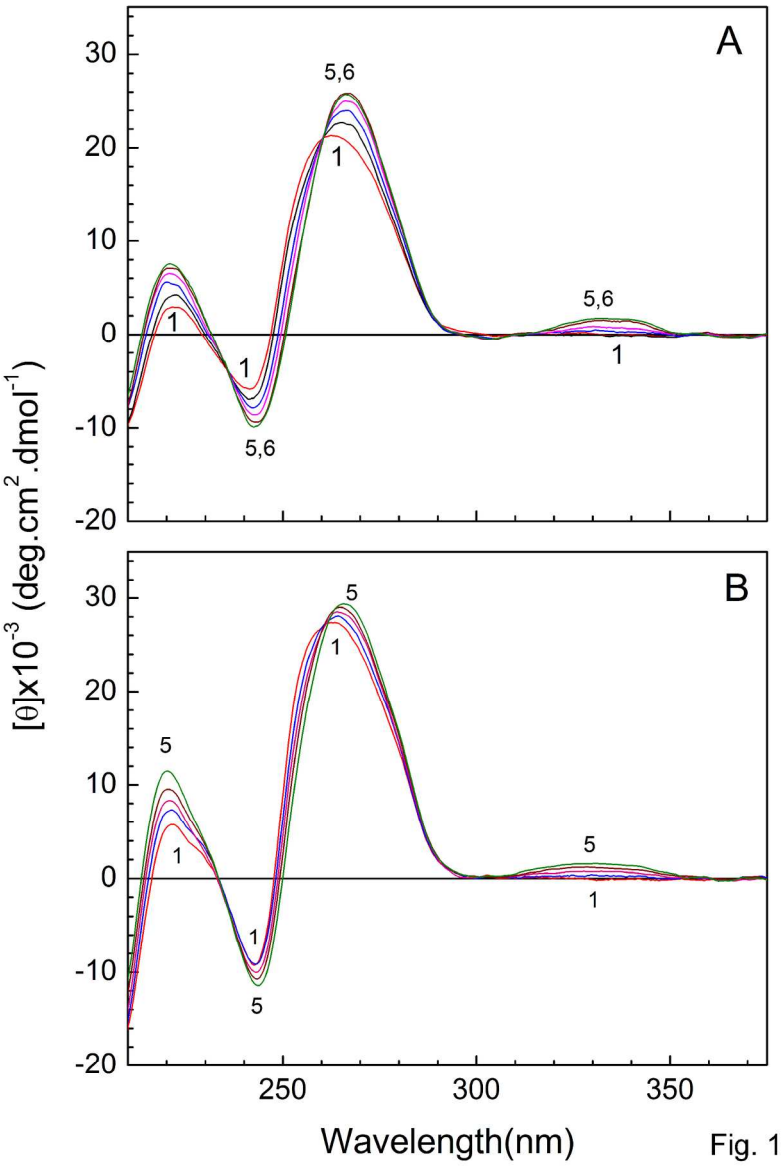

Fig. 10

176x245mm (300 x 300 DPI)

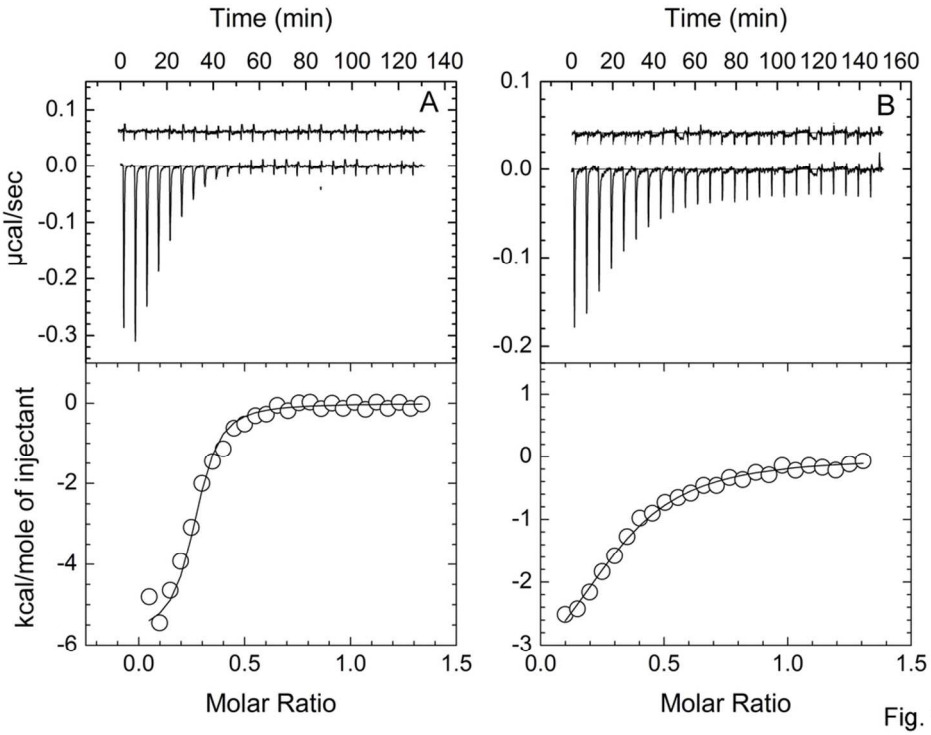

Fig. 11

97x75mm (300 x 300 DPI)